In-Cell Catalysis Hot Paper

How to cite: *Angew. Chem. Int. Ed.* **2021**, *60*, 4133–4141
International Edition: doi.org/10.1002/anie.202013366
German Edition: doi.org/10.1002/ange.202013366

Bioorthogonal Activation of Dual Catalytic and Anti-Cancer Activities of Organogold(I) Complexes in Living Systems

*Yan Long[+], Bei Cao[+], Xiaolin Xiong, Albert S. C. Chan, Raymond Wai-Yin Sun, and Taotao Zou**

Abstract: *Controllably activating the bio-reactivity of metal complexes in living systems is challenging but highly desirable because it can minimize off-target bindings and improve spatiotemporal specificity. Herein, we report a new bioorthogonal activation approach by employing Pd(II)-triggered transmetallation reactions to conditionally activate the bio-reactivity of NHC–Au(I)–phenylacetylide complexes (**1a**) in vitro and in vivo. A combination of ^{1}H NMR, LC-MS, DFT calculation and fluorescence screening assays reveals that **1a** displays a reasonable stability against biological thiols, but its phenylacetylide ligand can be efficiently transferred to Pd(II), leading to in situ formation of labile NHC–Au(I) species that is catalytically active inside living cells and zebrafish, and can meanwhile effectively suppress the activity of thioredoxin reductase, potently inhibit the proliferation of cancer cells and efficiently suppress angiogenesis in zebrafish models.*

Introduction

Gold(I) complexes have profound potential applications in biological systems by acting as anti-cancer drugs, biological catalysts and others.[1] These properties could mainly be accounted for by the "soft Lewis/π acid" nature of Au^+ ions.[2] However, the presence of large quantities of physiological nucleophiles (e.g., thiols) has posed a big hurdle for their bioapplications in vitro and in vivo because the nucleophiles can competitively bind and deactivate/poison gold(I) before reaching the target sites.[1h] This issue is particularly severe when developing gold(I) anti-cancer drugs since the non-specific binding with serum thiols and on-target inhibition of intracellular thiol-enzymes are both related to the thiol-reactivity of gold(I).[1c,e,h,3] In past years, tremendous efforts have been made by introducing ligands with variable donor strength to generate gold complexes having suitable thiol-reactivities.[3,4] Among these endeavors, strong σ donor ligands such as N-heterocyclic carbene (NHC),[5] phosphine,[6] and alkyne[7] have attracted particular attention due to their ability to improve the stability of gold while keeping enzyme-inhibiting activities. However, it still remains a big challenge to controllably deliver active gold(I) to the target site with high spatiotemporal selectivity.

Transition metal-mediated bioorthogonal activation is a powerful strategy to highly selectively convert inactive prodrugs, profluorophores or caged proteins into active forms via spatial and temporal administration of chemical inducers.[8] Notable reactions include uncaging,[9] cross coupling,[10] transfer hydrogenation,[11] reduction,[12] cycloaddition,[13] isomerization[14] etc. Nonetheless, the repertoire of bioorthogonal reactions, especially for transformations in living cells or animals, is far from the limit. In the literature, organometallic transmetallation is known to be a key step in cross coupling reactions by transferring alkynyl, aryl, vinyl etc., groups to metal catalysts (e.g., Pd).[15] In this process, strong metal-carbon bonds in the substrates are broken down, producing labile metal-ligand species. In view that organogold(I) complexes display a reasonably high stability under physiological conditions and can potentially undergo transmetallation reaction,[15,16] we conceive the possibility to conditionally activate gold(I) complexes by bioorthogonal transmetallation. We herein report that Pd(II) can efficiently trigger transmetallation reaction and activate organogold(I) in living systems, leading to forming active gold(I) species that can catalyze π-bond activation reactions and induce anti-cancer activities inside living cells and zebrafish in a highly controllable manner. To the best of our knowledge, this is the first example of using bioorthogonal activation approach to modulate the biological activity of gold complexes in living systems.

[*] Y. Long,[+] Dr. X. Xiong, Prof. Dr. A. S. C. Chan, Prof. Dr. T. Zou
Guangdong Provincial Key Laboratory of Chiral Molecule and Drug Discovery, Guangdong Provincial Key Laboratory of New Drug Design and Evaluation, School of Pharmaceutical Sciences, Sun Yat-Sen University
Guangzhou 510006 (P. R. China)
E-mail: zoutt3@mail.sysu.edu.cn

Dr. B. Cao[+]
Warshel Institute for Computational Biology, and General Education Division, The Chinese University of Hong Kong
Shenzhen 518172 (P. R. China)

Prof. Dr. R. W.-Y. Sun
Guangzhou Lee & Man Technology Company Limited
Guangzhou 510000 (P. R. China)

Prof. Dr. T. Zou
State Key Laboratory of Coordination Chemistry, Nanjing University
Nanjing 210093 (P. R. China)

Prof. Dr. T. Zou
State Key Laboratory for Chemistry and Molecular Engineering of Medicinal Resources, Guangxi Normal University
Guilin 541004 (P. R. China)

[+] These authors contributed equally to this work.

Supporting information and the ORCID identification number(s) for the author(s) of this article can be found under: https://doi.org/10.1002/anie.202013366.

Results and Discussion

Synthesis, stability and transmetallation reaction of gold(I) complexes

Since certain NHC–gold(I)-alkyne complexes have been reported to display high stability against thiols,[17] we prepared analogue complexes by employing imidazole-based carbene ligands and phenylacetylide or phenyl ligands to generate organometallic complexes of **1a**, **1b** and **1c** containing two Au–C bonds (Figure 1, see details of synthesis and characterization in the Supporting Information). Complexes **1a**–**1c** are

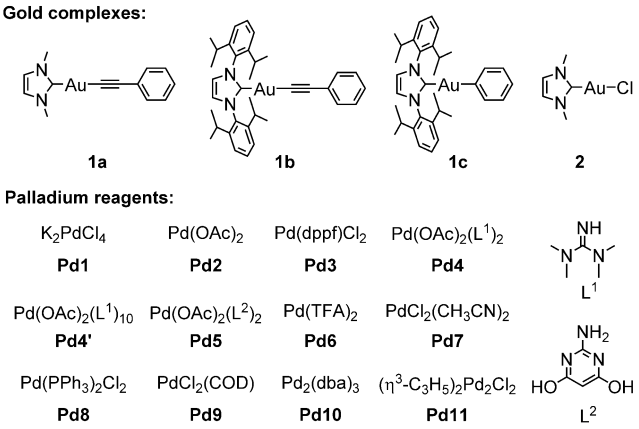

Figure 1. Chemical structures of gold complexes and the formula of Pd(II) reagents used in this work.

highly soluble ($>10\ mg\,mL^{-1}$) in common organic solvents such as DMSO, DMF, CH_2Cl_2, EtOH, and acetone, and can be dissolved in water after dilution from DMSO stock solutions (**1a** shows the highest solubility, $>300\ \mu M$ in 1 % DMSO). We initially tested the stability of these complexes towards biorelevant thiols. After incubating **1a** (8.5 mM) with 5-fold of N-acetyl cysteine (NAC) for 48 h in [D_6]DMSO, ^{1}H NMR showed no obvious change of ^{1}H signals of **1a** (Figure 2b). By using phosphate-buffered saline (PBS, pH 7.4, containing 20 % DMSO) as a solvent, **1a** (100 μM) also did not form new species with glutathione (GSH, 2 mM) after 48 h incubation as revealed from HPLC analysis (Figure S1). After incubating **1a** (100 μM) with living non-small cell lung cancer A549 cells for 10 h, followed by aspiration of medium, washing and cell lysis, we detected a significant amount of intact complex in the supernatant of cell lysates after acetone precipitation by HPLC analysis (Figure S2), suggesting that **1a** has a good stability against physiological thiols. Complex **1b** displays comparable stability (Figure S3), whereas **1c** slowly reacted with NAC based on ^{1}H NMR analysis (Figure S4).

Then we tested if **1a** could undergo transmetallation reaction by co-incubating with **Pd1**. Noticeably, once mixing **1a** with **Pd1** (1:1 ratio) in [D_6]DMSO, instant color change from yellow to dark brown was observed. ^{1}H NMR (Figure 2b) showed that the aromatic proton of phenylacetylene (7.15–7.28) dramatically disappeared, accompanied with downfield shift of $CH_{(Im)}$ from 7.39 ppm to 7.42 ppm and

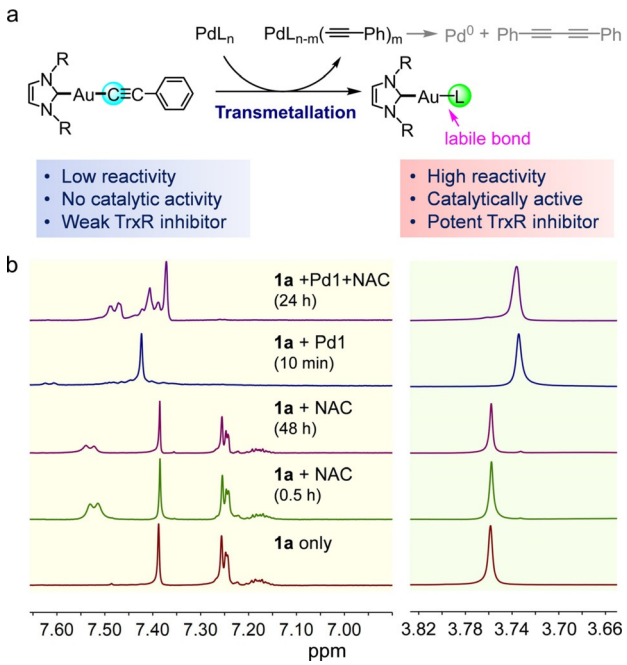

Figure 2. a) Pd(II)-triggered transmetallation effectively activated the reactivity of **1a** ($m=1$, 2). b) ^{1}H NMR of **1a** (8.5 mM) in the absence or presence of NAC (5 equiv.), or **Pd1** (1 equiv.), or **Pd1** (1 equiv.) + NAC (5 equiv.) for the indicated time in [D_6]DMSO. NAC was neutralized by equal amount of Et_3N in each condition.

upfield shift of N-CH_3 from 3.76 ppm to 3.73 ppm, and the shifted signals matched well with that of NHC-Au-Cl (**2**, Figure S5), suggestive of efficient transmetallation of metal-alkyne which is consistent with the literature report.[15,16] Additionally, HPLC analysis showed formation of 1,4-diphenylbuta-1,3-diyne (dpby) as the major product containing phenyl moiety (detected at OD_{254nm}, Figure S6) and X-ray photoelectron spectroscopy (XPS) experiments revealed generation of Pd^0 species (Figure S7), suggesting that the Pd(II)-alkyne underwent further reductive elimination.

Notably, transmetallation reaction also happened when 5-fold NAC was present in the mixture of **1a** and **Pd1**, though the full conversion requires a longer time (completed within 24 h, Figure 2b). Again, changing the solvents to PBS/DMSO (80:20 v/v) did not influence the reaction efficiency: HPLC analysis showed that **1a** (100 μM) was fully converted in 10 min with **Pd1** (100 μM, Figure S8), and it completely reacted with **Pd1** as well in the presence of GSH (2 mM, Figure S9) in 24 h. Complex **1a** reacted with other Pd(II) compounds such as **Pd2**, **Pd6** in a similar efficiency (Figure S10, S11). These results collectively indicate that Pd(II) can efficiently trigger transmetallation reaction to break Au-C(acetylide) bond under physiological-like conditions.

DFT calculations on the reaction mechanisms

To elaborate the possible mechanism of transmetallation process, density functional theory (DFT) calculations were performed at wb97XD level using basis-sets of LanL2DZ for Au and Pd atoms and 6–31 + G(2df) for other atoms, which

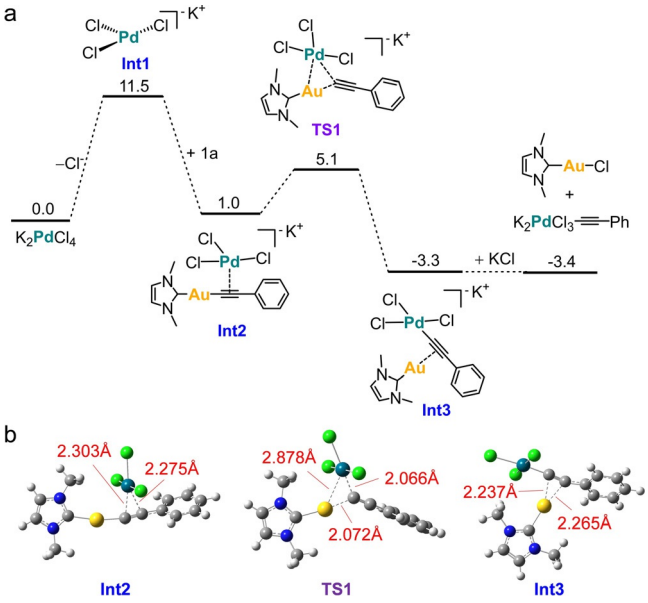

Figure 3. DFT calculations for the reactions between **1a** and **Pd1**: a) The computed reaction pathway and free energies of the transmetallation reaction. b) Computed structures of key reaction intermediates and transition state.

indicates a stepwise mechanism (Figure 3). The reaction is initiated by releasing a chloride ion from **Pd1** which consumes free eneygy of +11.5 kcal mol^{-1}, leaving a vacant orbital in **Int1** that favors the binding with phenylacetylide moiety of **1a** (−10.5 kcal mol^{-1}) via π bonding (Figure 3b). Then **Int2** isomerizes to a 3-centered transition state (**TS1**) featuring an Au-Pd-C triangule geometry, where the Au-Pd distance is 2.878 Å that is shorter than the sum of Au + Pd van der Waals radii (3.29 Å).[18] This metal-metal interaction stablizes the transition state, leading to a rather small energy barrier (+4.1 kcal mol^{-1}). **TS1** is followed by the events of Au−C bond breaking to form **Int3** in which the terminal carbon of phenylacetylene is coordinated to Pd whereas the NHC-Au moiety is weakly bound to the triple bond via metal-π interaction (Figure 3b), finally leading to formation of labile NHC-Au-Cl.

By contrast, **1a** reacts with NAC more endothermically. Initial attempts to locate a transition state via a direct thiol to gold-phenylacetylide nucleophilic addition in a trigonal-planar geometry failed, despite of using different functionals and basis sets. Instead, we found a transition state (**TS1′**) featuring a proton transfer process from thiol to terminal phenylacetylene (Figure S12) by consuming an energy as high as +29.4 kcal mol^{-1}, followed by releasing phenylacetylene and generating NHC-Au-S(NAC) product. This energy barrier is much higher than that in the transmetallation process and agrees with the stability test as shown above.

Turning on the catalytic activity of gold(I) in buffer solutions

Since palladium-mediated transmetallation generates labile NHC-gold(I) species that is potentially active for catalysis, we tested its ability for π-bond activation by using a coumarin precursor as substrates (probe-1, Figure 4a). After incubating the mixture of **1a** (20 μM), probe-1 (100 μM) and different Pd(II) reagents (40 μM, 2-equivalent of **1a** to ensure complete transmetallation) for 1 h in CH_3CN, remarkable emission increase (peaked at 530 nm) was detected in the case of **Pd6** ($Pd(TFA)_2$, TFA = trifluoroacetate) by >1000-fold compared to probe-1 (yield = 52%), though **Pd6** itself also triggered 5% yield of background emission (Figure S13, but **1a** alone could not induce emission enhancement). However, **1a** with other Pd(II) compounds cannot trigger similar emission increment (Figure S13), which may be due to the auxiliary ligands (such as Cl^- and OAc^-) transferred back from Pd(II) deactivated gold catalysts. In fact, NHC-Au-Cl (**2**) is inactive to catalyze the cyclization reaction in CH_3CN.

Interestingly, addition of 50% volume of water in acetonitrile elevated the catalytic activity of **2** (Figure S14) with ≈33-fold increase of emission intensity after 1 h (yield 3%. Note: the emission intensity of coumarin varies in different solvents). This result is consistent with the previous report showing that water can help liberate Au-Cl bond and form active catalysts.[19] Notably, "**1a** + **Pd1**" also became catalytic active in CH_3CN/H_2O (1/1 v/v), with 675-fold increase in emission intensity (yield 66%, TON 3.3) in 1 h which is 20-fold higher than that by **2** (Figure S14). Complete conversion of 0.05 mmol of probe-1 was identified after 24 h catalyzed by 10% mol "**1a** + 10% mol **Pd1**" (isolated yield 78%, TON 7.8) in CH_3CN/H_2O (1/1 v/v). Based on this phenomenon, we speculate to use fluorescence measurement as a screening method to study the transmetallation efficiency in aqueous media. After incubating the mixture of **1a** (20 μM) + Pd(II) (40 μM) and probe-1 (100 μM) for 1 h in CH_3CN/H_2O (1/1 v/v), we detected emission enhancement in 11 out of 12 Pd reagents (green column, Figure 4c, except **Pd5** which needs a longer reaction time), and "**1a** + **Pd9**" generated the highest emission intensity (yield 96%, TON 4.8). It is noteworthy that the intensity of "**1a** + Pd" is generally higher than the similar condition by Pd(II) (red column, Figure 4c). The insoluble Pd^0-containing precipitate (Pd^0-iso) isolated from the reaction of "**1a** + **Pd1**" triggered <2% yield that is comparable to **Pd1**; other Pd reagents such as the species generated from "**1a** + phenylene + Et_3N" (Pd^0-prep, characterized by HPLC and XPS, Figure S15a,b), Pd/alkyne species generated in situ by transmetallation from [Cu^I(C≡C-Ph)] to **Pd1**, $Pd^0_2(dba)_3$, $Pd^0(PPh_3)_4$, Pd^0/C, and *trans*-Pd(II)-$(PPh_3)_2Cl$(C≡C-Ph) all induced <3% yield (Figure S16), suggesting that the active catalyst is Pd(II)-activated gold(I). Complexes **1b** and **1c** display comparable activity (Figure 4c). Replacing the solvent to PB (without Cl^-) or PBS (containing 137 mM of Cl^-) attenuated the catalytic efficiency but the background emission induced by Pd(II) was much weaker (Figure 4b,d). By comparing the intensity ratio of "Au + Pd" $I_{(Au+Pd)}$ and "Pd alone" $I_{(Pd)}$ (Figure 4d), **1a** in PBS was found to display the highest ratio in the presence of 6 out of 12 Pd(II) compounds (**Pd1**, **Pd3**, **Pd6**, **Pd7**, **Pd8**, **Pd10**, Figure 4d). These results indicate that Pd(II)-triggered transmetallation works efficiently and the as-formed gold species is catalytically active for π-bond activation under buffer conditions.

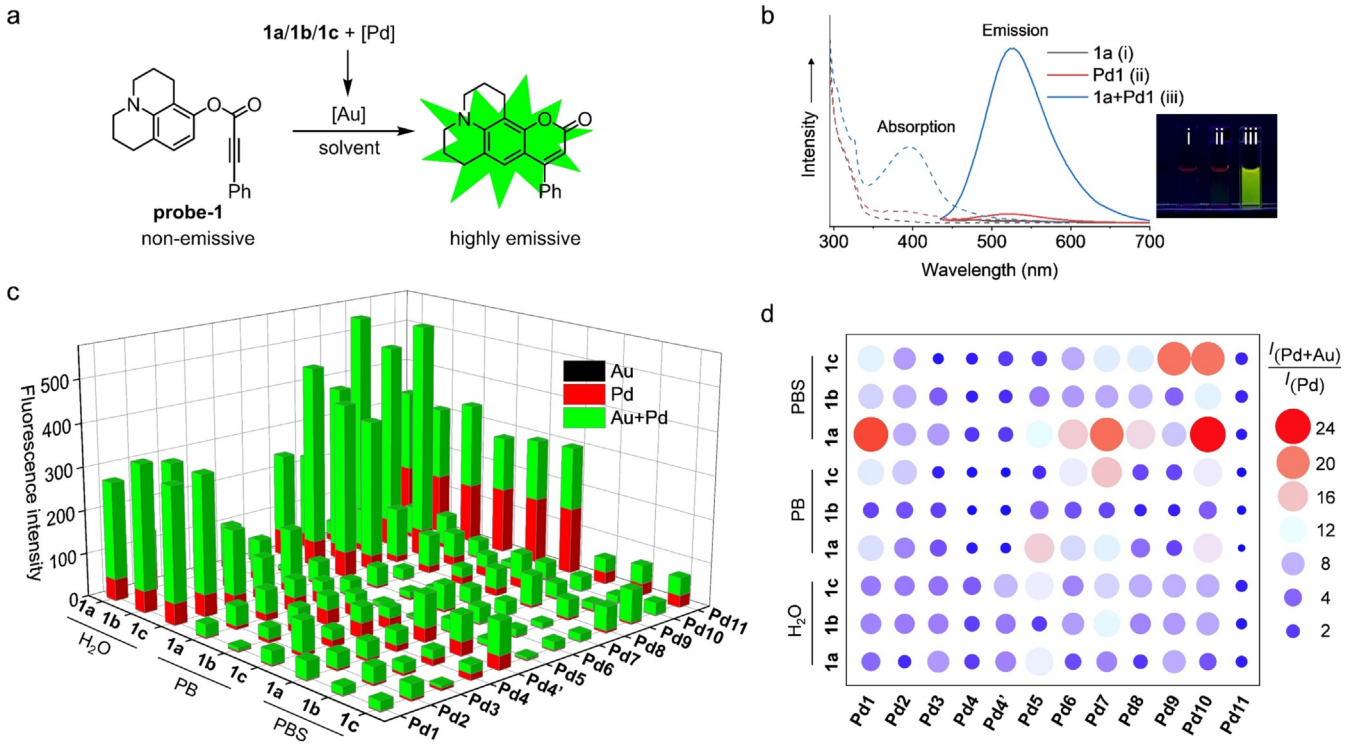

Figure 4. Screening of active Pd(II) reagents. a) Pd(II)-activated NHC-gold(I) species catalyzed the cyclization of probe-1 to form fluorescent coumarin. b) Absorption and emission spectra of probe-1 (100 μM) after treatment by **1a** (20 μM), **Pd1** (40 μM), or **1a** (20 μM) + **Pd1** (40 μM) for 1 h in CH_3CN/PBS (1:1) solution. c) Emission intensity (I_{530nm}) of probe-1 (100 μM) and organogold(I) (20 μM) in the presence of different Pd(II) reagents (40 μM) in solution of H_2O, PB or PBS after 1 h (except **Pd5** for 24 h). An equal volume of CH_3CN was added in each case to ensure all the reactants/products are soluble in the reaction mixture. d) Ratio (I_{Pd+Au}/I_{Pd}) of emission intensity of probe-1 in the presence of Pd + Au and Pd.

Activating the catalytic activity of gold(I) inside cancer cells

In the literature, physiological thiols have been reported to poison gold catalysts. Indeed, we found **2** (100 μM), in the presence of an equal amount of GSH, lost its catalytical activity with < 5-fold emission increase in aqueous solution (Figure S17). Surprisingly, "**1a** (100 μM) + **Pd1** (100 μM)" still displayed a good activity with 95-fold emission enhancement in the presence of 100 μM of GSH (Figure S17), and maintained 65-fold emission increase when 5-equivalent of GSH (500 μM) was present (Figure S18, **Pd1** alone triggered < 5-fold emission increase), indicating that the transmetallation–activation approach could minimize the influence of thiols for gold catalysis.

Then we examined if this reaction would take place in living cells. Here **Pd4** was used because it displays a low cytotoxicity (IC_{50} > 500 μM, 24 h) and is catalytically active. A549 cells were first treated with 100 μM of probe-1 (cytotoxic IC_{50} > 500 μM, 24 h) for 5 h. Then the medium was aspirated, and the cells were rinsed with PBS to wash out extracellular probes. Subsequently, fresh medium containing "**1a** + **Pd4**", or "**1a**", or "**Pd4**" was added for another 1 h incubation. The cells were imaged after replacing the medium with PBS (Figure 5a). As shown in Figure 5b, while only weak emission was detected in the treatment group by **1a** or **Pd4** alone, remarkable green emission was detected in A549 cells by "**1a** + **Pd4**" co-treatment, which is mainly localized in cytoplasmic regions (Figure S19). The treatment did not cause obvious cytotoxicity as revealed from the intact cell morphology (Figure 5b, S16). For comparison, complex **2** and the Pd^0 species (Pd^0-iso and Pd^0-prep) did not induce noticeable emission at the similar treatment condition (Figure S20, S21). These results collectively indicate that Pd(II)-triggered transmetallation is an effective strategy to activate in-cell gold catalysis.

Boosting the thiol-reactivity and anti-cancer activity of gold(I) by transmetallation

In view that Pd(II) can efficiently trigger transmetallation inside cancer cells, the activated gold(I) species is expected to inhibit cellular thiol- and/or selenol-containing enzymes (e.g., thioredoxin reductase, TrxR, a flavin enzyme containing cysteine and selenocysteine residues at C-terminus[1c,d,h]) and induce cytotoxicity after a longer incubation time. Indeed, it was found despite that treating A549 cells with **1a** or **Pd4** for 1 h did not show obvious TrxR inhibition (IC_{50} > 100 μM), addition of **Pd4** significantly increased the inhibitory activity of **1a** to an IC_{50} value of 14.8 ± 3.5 μM that is ≈7-fold higher than **1a** alone and is more potent than compound **2** (IC_{50} = 24.0 ± 2.3 μM). Other Pd(II) compounds such as **Pd1**, **Pd2**, and **Pd4'** could also activate **1a** with TrxR inhibitory IC_{50} of 14.1–27.0 μM (Table S1). Then we tested if the Pd(II) com-

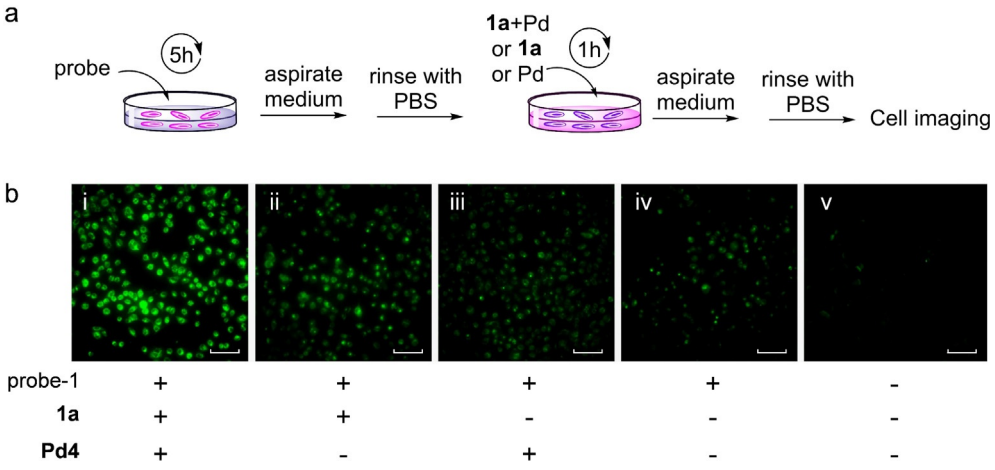

Figure 5. Activating the cellular catalytic activity of **1a** by Pd(II) reagents: a) A549 cells were treated with 100 μM probe-1 for 5 h, and then the medium was aspirated followed by washing with PBS twice; after that the cells were treated **1a** (100 μM) + **Pd4** (300 μM) or **1a** (100 μM) or **Pd4** (300 μM) for 1 h before the cells were washed and exposed for cell imaging. b) Fluorescence images of A549 cells after treatment by the above conditions (ex: 480 ± 15 nm, em: 535 ± 20 nm). Scale bar: 100 μm.

pounds could serve as a trigger for the cytotoxicity of gold(I) complexes. Initial test by using **Pd4** showed that the cytotoxicity IC_{50} of **1a**, after adding the Pd(II) salt, increased from 63.3 to 17.5 μM towards A549 cells. The other two non-toxic Pd(II) compounds **Pd4′** and **Pd5** could induce a slightly higher cytotoxicity to IC_{50} values of 13.1 μM (Table 1). We also tested their cytotoxicity towards human hepatocellular carcinoma HepG2, breast cancer MCF-7 and glioblastoma U87 cells. Again, **1a** alone displayed low cytotoxicity, with IC_{50} of 52.4 to 70.6 μM. Addition of **Pd4′** and **Pd5** significantly increased the cytotoxicity to 8.5–13.1 μM and 6.4–18.5 μM, respectively. Complex **1b** could be activated in a comparable potency by **Pd4′** and **Pd5** with notable cytotoxicity improvement in HepG2 (from 84.0 μM to 8.5 μM) and A549 (from 36.6 μM to 4.4 μM) cells after **Pd4′** co-treatment (Table S2). For comparison, the cytotoxicity of **2** was marginally increased with IC_{50} value from 48.1 μM to 19.4 μM after **Pd4′** co-treatment. Also, Pd^0-iso and Pd^0-prep are non-toxic (IC_{50} > 100 μM) and dpby displays low cytotoxicity (IC_{50} = 81.3 μM). These results reveal that Pd(II) is able to activate the thiol-reactivity and cytotoxicity of organogold(I) complexes (**1a** and **1b**) in cancer cells. In addition, "**1a** + **Pd1**" effectively induced ROS formation as revealed from DCFH-CA staining (Figure S22) and initiated apoptosis according to Annexin V-FITC/PI co-staining assay (Figure S23), which

Table 1: Cytotoxicity IC_{50} (μM) of **1a** in the presence/absence of **Pd4′** or **Pd5** towards HepG2, A549, MCF-7 and U87 cells after 72-h treatment.

Entry	**1a**	**1a** + **Pd4′**[a]	**1a** + **Pd5**[b]	**Pd4′**[c]	**Pd5**[c]
A549	63.3 ± 1.1	13.1 ± 2.8	13.1 ± 4.0	> 200	> 200
HepG2	70.6 ± 0.7	12.0 ± 3.6	18.5 ± 1.2	> 200	> 200
MCF-7	54.3 ± 0.2	11.8 ± 1.9	13.8 ± 0.3	> 200	> 200
U87	52.4 ± 0.2	8.5 ± 0.2	6.4 ± 1.8	> 200	> 200

[a] [**Pd4′**] = 200 μM. [b] [**Pd5**] = 200 μM; [c] The cell viability at 200 μM is > 90%.

are consistent with the TrxR inhibitory activity and cytotoxicity as shown before.

HRGDH-Pd for tumor-targeted drug activation

Based on the fact that Pd(II) is key to the cytotoxicity of organogold(I), we considered the possibility for cancer-specific drug activation by introducing tumor targeting groups into Pd(II) instead of gold(I).[20] It has been reported that peptides containing two His moieties at *i* and *i* + 4 positions could act as bidentate ligands to form catalytically active, stapled Pd(II) complexes.[21] Here we employed an RGD-containing peptide and prepared an **HRGDH-Pd** complex[21] for selective recognition and accumulation of Pd(II) in integrin-overexpressing cancer cells (Figure 6a,b).[22] MTT assay showed that **HRGDH-Pd** (50 μM) renders **1a** to display very different cytotoxicity towards integrin-high expressing HeLa cells[22a] and integrin-low expressing normal LO2 cells[22b] with cell viability of 22.0% and 79.6% respectively at 25 μM of **1a** (i.e., 3.8-fold improvement), and 2.6% and 59.0% respectively at 50 μM of **1a** (i.e., 12-fold improvement) after 48 h treatment (Figure 6c).

We further used a HeLa/LO2 co-culture experiment to examine the capability of "**1a** + **HRGDH-Pd**" for targeted activation in integrin-high expressing cancer cells (Figure 6d). The red-orange fluorescent tetramethyl-rhodamine (TMR) moiety tagged on **HRGDH-Pd** was used to indicate the cellular content/uptake of Pd(II), and the viable cells were distinguished by calcein AM staining which shows green emission after esterase cleavage in living cells. An equal number of HeLa and LO2 cells were co-cultured in a single dish and treated with **HRGDH-Pd** (100 μM) for 6 h; subsequently the medium was removed and replaced with fresh one containing of **1a** (100 μM) for a further 10 h incubation. The cells were treated with calcein AM for 30 min before cell imaging. As depicted in Figure 6d, near 50% of cells were stained with red color, indicative of efficient uptake of **HRGDH-Pd** in cancer cells. Notably, the red emission of most cancer cells could not overlay the green emission of living cells (dashed circle, upper panel, Figure 6d), indicating that the cells with high Pd(II) contents tend to die. For comparison, in the **HRGDH-Pd** treatment group without **1a**, the red fluorescent cells are merged well with the green emission of living cells (merged in yellow color, Figure 6d, lower panel), suggesting that the cytotoxicity after "**1a** + **HRGDH-Pd**" treatment is originated from Pd(II)-activated gold(I) rather than the Pd(II) compounds. Therefore, it is indeed possible

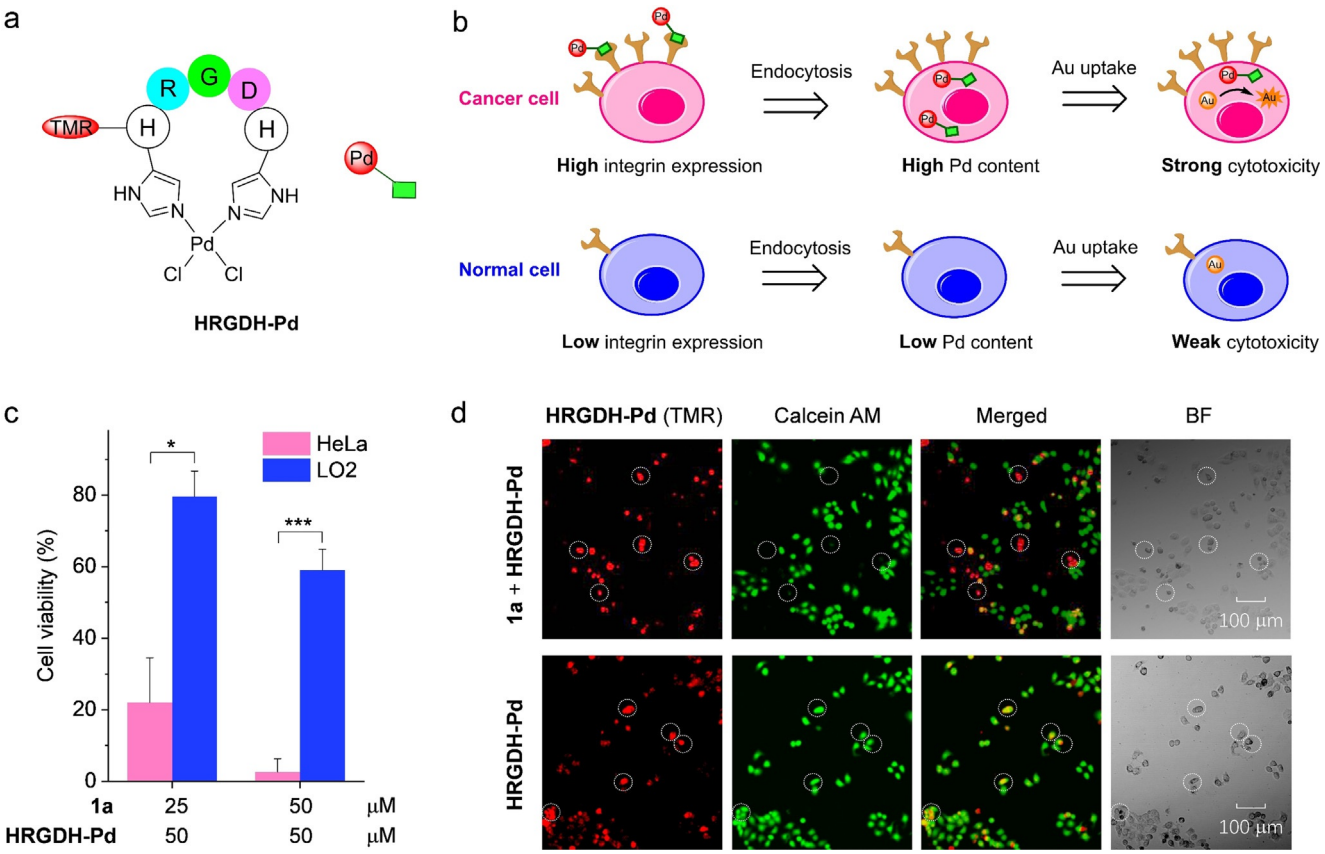

Figure 6. Targeted drug activation: a) Structure of **HRGDH-Pd** which contains a red-orange fluorescent TMR tag. b) Proposed mechanism for targeted drug activation by selective accumulation of Pd(II) in integrin-overexpressing cancer cells followed by transmetallation activation on the cytotoxicity of **1a**. c) The viability of HeLa and LO2 cells after treatment by **HRGDH-Pd** (50 μM) for 6 h and then **1a** (25 or 50 μM) for 48 h. * $p<0.05$, *** $p<0.001$. d) The co-cultured HeLa/LO2 cells were treated with **HRGDH-Pd** (100 μM) for 6 h; then the medium was aspirated and replaced with fresh one containing **1a** (100 μM) for a further 10 h incubation. The cells were imaged after adding calcein AM for 30 min. Red channel: ex 561 nm, em 576–626 nm; green channel: ex 488, em 500–540 nm.

for gold complexes to distinguish between cancer and normal cells by using functionalized Pd(II) for drug activation.

Bioorthogonal activation in zebrafish models

To investigate if transmetallation activation works under in vivo conditions, wild type zebrafish (AB) were treated with **Pd4** (10 μM) for 2 h, the culture solution of which was then removed followed by adding an equal molar of **1a** (10 μM) and probe-1 for another 1 h incubation. Fluorescence microscopic analysis showed highly bright green emission in zebrafish by "**1a** + **Pd4** + probe-1" co-treatment (Figure 7a, mainly in head and belly region), whereas the fluorescence was much weaker in the absence of either **1a** or **Pd4** or "**1a** + **Pd4**". A lower concentration of "**1a** + Pd" could also induce significant emission increase (Figure S24).

As reported before, zebrafish is a good model to study tumor angiogenesis and certain thiol-reactive gold(I) complexes can inhibit angiogenesis in this model.[4e,7b] We employed a GFP-flk transgenic zebrafish model, which shows green fluorescence in vasculature, to examine whether the activated gold(I) is able to inhibit angiogenesis. The zebrafish embryos were incubated with **1a** and/or **Pd4** and the fluorescence images were captured three days post fertilization. As depicted in Figure 7b, "**1a** + **Pd4**" co-treatment significantly impaired the vascular structures of zebrafish

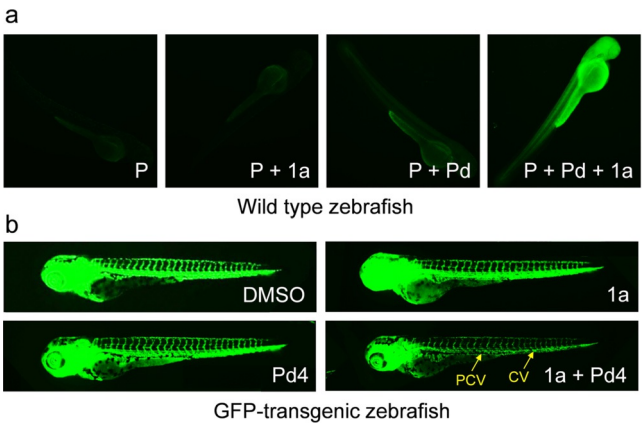

Figure 7. a) Fluorescence images of wild type zebrafish treated with **Pd4** (10 μM) for 2 h, followed by replacing culture solution with fresh one containing **1a** (10 μM) and probe-1 (P, 10 μM) for another 1 h incubation. b) Blood vessel formation during zebrafish embryo development after treatment by **1a** (10 μM), **Pd4** (20 μM) or "**1a** (10 μM) + **Pd4** (20 μM)". The images were taken 3 days after fertilization.

particularly in posterior cardinal vein (PCV) and caudal vein (CV) regions. For comparison, single **1a** or **Pd4** treatment did not obviously damage blood vessel formation, implying that the activated gold(I) species is indeed active for anti-angiogenesis.

Conclusion

In summary, we have developed a novel bioorthogonal activation approach that can transform stable organogold(I) complexes into active gold(I) inside living systems in a controllable manner. This approach is based on a combination of using organogold(I) complexes with a reasonable stability and using palladium(II)-triggered transmetallation reactions for gold(I) activation. The organogold(I) complex remains in an "off" state before being activated by Pd(II) salts. The in situ activation, on the one hand, renders gold(I) with high catalytic activity for π-bond activation via forming highly fluorescent coumarin inside living cells and zebrafish. The Pd(II) compounds, on the other hand, boosted the thiol-reactivity of gold(I) to suppress the cellular activity of thioredoxin reductase and to inhibit the proliferation of cancer cells, along with potent anti-angiogenesis in zebrafish models. It is noteworthy that RGD-functionalized Pd(II) can selectively activate organogold(I) and convey cytotoxicity in integrin-overexpressing cancer cells over normal cells, thus providing an opportunity for targeted tumor therapy via site-specific delivery of Pd(II) rather than direct ligand modification on gold(I) drugs.

In the literature, gold(I) is known to have profound applications in organic catalysis and is also known as potent thiol-enzyme inhibitors, but their applications in vitro and in vivo are largely hampered by off-target interactions. We believe our approach offers an opportunity to minimize off-target bindings and improve spatiotemporal specificity by bioorthogonal activation that can be tuned for a broad spectrum of biological applications.

Acknowledgements

T.Z. acknowledges the support from Guangdong Science and Technology Department (No. 2019QN01C125). This work was financially supported by the start-up funding of Sun Yat-Sen University, Fundamental Research Funds for the Central Universities (19ykjc02), Guangdong Provincial Key Lab of Chiral Molecule and Drug Discovery (2019B030301005), Guangdong Provincial Key Laboratory of Construction Foundation (2017B030314030, 2020B1212060034), Shenzhen Fundamental Research Fund JCYJ20180508163206306, the open project from the State Key Laboratory of Coordination Chemistry in Nanjing University and the State Key Laboratory for Chemistry and Molecular Engineering of Medicinal Resources in Guangxi Normal University (CMEMR2020-B01), Guangdong Province Zhu Jiang Talents Plan (2016ZT06C090) and Guangzhou City Talents Plan (CYLJTD-201609). The Warshel Institute for Computational Biology funding from Shenzhen City and Long-gang District is also acknowledged.

Conflict of interest

The authors declare no conflict of interest.

Keywords: anti-cancer · bioorthogonal activation · gold medicine · in-cell catalysis · thiol reactivity

[1] a) P. J. Sadler, R. E. Sue, *Met.-Based Drugs* **1994**, *1*, 107–144; b) C. F. Shaw III, *Chem. Rev.* **1999**, *99*, 2589–2600; c) I. Ott, *Coord. Chem. Rev.* **2009**, *253*, 1670–1681; d) S. Nobili, E. Mini, I. Landini, C. Gabbiani, A. Casini, L. Messori, *Med. Res. Rev.* **2010**, *30*, 550–580; e) S. J. Berners-Price, A. Filipovska, *Metallomics* **2011**, *3*, 863–873; f) N. J. Farrer, P. J. Sadler in *Bioinorg. Med. Chem.* (Ed.: E. Alessio), Wiley-VCH, Weinheim, **2011**, pp. 1–37; g) N. Muhammad, Z. Guo, *Curr. Opin. Chem. Biol.* **2014**, *19*, 144–153; h) T. Zou, C. T. Lum, C.-N. Lok, J.-J. Zhang, C.-M. Che, *Chem. Soc. Rev.* **2015**, *44*, 8786–8801; i) A. Ssemaganda, L. M. Low, K. R. Verhoeft, M. Wambuzi, B. Kawoozo, S. B. Nabasumba, J. Mpendo, B. S. Bagaya, N. Kiwanuka, D. I. Stanisic, S. J. Berners-Price, M. F. Good, *Metallomics* **2018**, *10*, 444–454; j) M. Mora, M. C. Gimeno, R. Visbal, *Chem. Soc. Rev.* **2019**, *48*, 447–462; k) S. R. Thomas, A. Casini, *Curr. Opin. Chem. Biol.* **2020**, *55*, 103–110.

[2] a) Z. Du, R. E. F. de Paiva, K. Nelson, N. P. Farrell, *Angew. Chem. Int. Ed.* **2017**, *56*, 4464–4467; *Angew. Chem.* **2017**, *129*, 4535–4538; b) A. Giorgio, A. Merlino, *Coord. Chem. Rev.* **2020**, *407*, 213175.

[3] Z. Yang, G. Jiang, Z. Xu, S. Zhao, W. Liu, *Coord. Chem. Rev.* **2020**, *423*, 213492.

[4] a) P. J. Barnard, L. E. Wedlock, M. V. Baker, S. J. Berners-Price, D. A. Joyce, B. W. Skelton, J. H. Steer, *Angew. Chem. Int. Ed.* **2006**, *45*, 5966–5970; *Angew. Chem.* **2006**, *118*, 6112–6116; b) V. Milacic, D. Chen, L. Ronconi, K. R. Landis-Piwowar, D. Fregona, Q. P. Dou, *Cancer Res.* **2006**, *66*, 10478–10486; c) C. Marzano, L. Ronconi, F. Chiara, M. C. Giron, I. Faustinelli, P. Cristofori, A. Trevisan, D. Fregona, *Int. J. Cancer* **2011**, *129*, 487–496; d) W. Liu, R. Gust, *Coord. Chem. Rev.* **2016**, *329*, 191–213; e) H. Luo, B. Cao, A. S. C. Chan, R. W.-Y. Sun, T. Zou, *Angew. Chem. Int. Ed.* **2020**, *59*, 11046–11052; *Angew. Chem.* **2020**, *132*, 11139–11145.

[5] a) J. L. Hickey, R. A. Ruhayel, P. J. Barnard, M. V. Baker, S. J. Berners-Price, A. Filipovska, *J. Am. Chem. Soc.* **2008**, *130*, 12570–12571; b) S. Ray, R. Mohan, J. K. Singh, M. K. Samantaray, M. M. Shaikh, D. Panda, P. Ghosh, *J. Am. Chem. Soc.* **2007**, *129*, 15042–15053; c) W. Liu, R. Gust, *Chem. Soc. Rev.* **2013**, *42*, 755–773; d) F. Cisnetti, A. Gautier, *Angew. Chem. Int. Ed.* **2013**, *52*, 11976–11978; *Angew. Chem.* **2013**, *125*, 12194–12196; e) T. Zou, C. T. Lum, C.-N. Lok, W.-P. To, K.-H. Low, C.-M. Che, *Angew. Chem. Int. Ed.* **2014**, *53*, 5810–5814; *Angew. Chem.* **2014**, *126*, 5920–5924; f) W. Niu, X. Chen, W. Tan, A. S. Veige, *Angew. Chem. Int. Ed.* **2016**, *55*, 8889–8893; *Angew. Chem.* **2016**, *128*, 9035–9039; g) C. Bazzicalupi, M. Ferraroni, F. Papi, L. Massai, B. Bertrand, L. Messori, P. Gratteri, A. Casini, *Angew. Chem. Int. Ed.* **2016**, *55*, 4256–4259; *Angew. Chem.* **2016**, *128*, 4328–4331; h) J. Fernández-Gallardo, B. T. Elie, M. Sanaú, M. Contel, *Chem. Commun.* **2016**, *52*, 3155–3158; i) T. Zou, C.-N. Lok, P.-K. Wan, Z.-F. Zhang, S.-K. Fung, C.-M. Che, *Curr. Opin. Chem. Biol.* **2018**, *43*, 30–36; j) C. Zhang, P.-Y. Fortin, G. Barnoin, X. Qin, X. Wang, A. Fernandez Alvarez, C. Bijani, M.-L. Maddelein, C. Hemmert, O. Cuvillier, H. Gornitzka, *Angew. Chem. Int. Ed.* **2020**, *59*, 12062–12068; *Angew. Chem.* **2020**, *132*,

12160 – 12166; k) F. Guarra, A. Terenzi, C. Pirker, R. Passannante, D. Baier, E. Zangrando, V. Gómez-Vallejo, T. Biver, C. Gabbiani, W. Berger, J. Llop, L. Salassa, *Angew. Chem. Int. Ed.* **2020**, *59*, 17130 – 17136; *Angew. Chem.* **2020**, *132*, 17278 – 17284.

[6] a) S. J. Berners-Price, C. K. Mirabelli, R. K. Johnson, M. R. Mattern, F. L. McCabe, L. F. Faucette, C.-M. Sung, S.-M. Mong, P. J. Sadler, S. T. Crooke, *Cancer Res.* **1986**, *46*, 5486 – 5493; b) S. D. Köster, H. Alborzinia, S. Can, I. Kitanovic, S. Wölfl, R. Rubbiani, I. Ott, P. Riesterer, A. Prokop, K. Merz, N. Metzler-Nolte, *Chem. Sci.* **2012**, *3*, 2062 – 2072; c) B. T. Elie, J. Fernández-Gallardo, N. Curado, M. A. Cornejo, J. W. Ramos, M. Contel, *Eur. J. Med. Chem.* **2019**, *161*, 310 – 322; d) B. T. Elie, K. Hubbard, B. Layek, W. S. Yang, S. Prabha, J. W. Ramos, M. Contel, *ACS Pharmacol. Transl. Sci.* **2020**, *3*, 644 – 654.

[7] a) J. Carlos Lima, L. Rodríguez, *Chem. Soc. Rev.* **2011**, *40*, 5442 – 5456; b) A. Meyer, C. P. Bagowski, M. Kokoschka, M. Stefanopoulou, H. Alborzinia, S. Can, D. H. Vlecken, W. S. Sheldrick, S. Wölfl, I. Ott, *Angew. Chem. Int. Ed.* **2012**, *51*, 8895 – 8899; *Angew. Chem.* **2012**, *124*, 9025 – 9030; c) V. Fernández-Moreira, I. Marzo, M. C. Gimeno, *Chem. Sci.* **2014**, *5*, 4434 – 4446; d) J.-J. Zhang, M. A. Abu el Maaty, H. Hoffmeister, C. Schmidt, J. K. Muenzner, R. Schobert, S. Wölfl, I. Ott, *Angew. Chem. Int. Ed.* **2020**, *59*, 16795 – 16800; *Angew. Chem.* **2020**, *132*, 16940 – 16945.

[8] a) J. A. Prescher, C. R. Bertozzi, *Nat. Chem. Biol.* **2005**, *1*, 13 – 21; b) M. Yang, J. Li, P. R. Chen, *Chem. Soc. Rev.* **2014**, *43*, 6511 – 6526; c) T. Voelker, E. Meggers, *Curr. Opin. Chem. Biol.* **2015**, *25*, 48 – 54; d) J. J. Soldevila-Barreda, P. J. Sadler, *Curr. Opin. Chem. Biol.* **2015**, *25*, 172 – 183; e) Z. Yu, J. A. Cowan, *Chem. Eur. J.* **2017**, *23*, 14113 – 14127; f) M. Martínez-Calvo, J. L. Mascareñas, *Coord. Chem. Rev.* **2018**, *359*, 57 – 79; g) A. H. Ngo, S. Bose, L. H. Do, *Chem. Eur. J.* **2018**, *24*, 10584 – 10594; h) J. G. Rebelein, T. R. Ward, *Curr. Opin. Biotechnol.* **2018**, *53*, 106 – 114; i) J. J. Soldevila-Barreda, N. Metzler-Nolte, *Chem. Rev.* **2019**, *119*, 829 – 869; j) J. Ohata, S. C. Martin, Z. T. Ball, *Angew. Chem. Int. Ed.* **2019**, *58*, 6176 – 6199; *Angew. Chem.* **2019**, *131*, 6238 – 6264; k) S. Eda, I. Nasibullin, K. Vong, N. Kudo, M. Yoshida, A. Kurbangalieva, K. Tanaka, *Nat. Catal.* **2019**, *2*, 780 – 792; l) X. Wang, X. Wang, S. Jin, N. Muhammad, Z. Guo, *Chem. Rev.* **2019**, *119*, 1138 – 1192; m) S. Alonso-de Castro, A. Terenzi, J. Gurruchaga-Pereda, L. Salassa, *Chem. Eur. J.* **2019**, *25*, 6651 – 6660; n) X. Ji, Z. Pan, B. Yu, L. K. De La Cruz, Y. Zheng, B. Ke, B. Wang, *Chem. Soc. Rev.* **2019**, *48*, 1077 – 1094; o) F. Wang, Y. Zhang, Z. Liu, Z. Du, L. Zhang, J. Ren, X. Qu, *Angew. Chem. Int. Ed.* **2019**, *58*, 6987 – 6992; *Angew. Chem.* **2019**, *131*, 7061 – 7066; p) S. S. Nguyen, J. A. Prescher, *Nat. Rev. Chem.* **2020**, *4*, 476 – 489.

[9] a) C. Streu, E. Meggers, *Angew. Chem. Int. Ed.* **2006**, *45*, 5645 – 5648; *Angew. Chem.* **2006**, *118*, 5773 – 5776; b) J. T. Weiss, J. C. Dawson, K. G. Macleod, W. Rybski, C. Fraser, C. Torres-Sánchez, E. E. Patton, M. Bradley, N. O. Carragher, A. Unciti-Broceta, *Nat. Commun.* **2014**, *5*, 3277; c) J. Li, J. Yu, J. Zhao, J. Wang, S. Zheng, S. Lin, L. Chen, M. Yang, S. Jia, X. Zhang, P. R. Chen, *Nat. Chem.* **2014**, *6*, 352 – 361; d) T. Völker, F. Dempwolff, P. L. Graumann, E. Meggers, *Angew. Chem. Int. Ed.* **2014**, *53*, 10536 – 10540; *Angew. Chem.* **2014**, *126*, 10705 – 10710; e) G. Y. Tonga, Y. Jeong, B. Duncan, T. Mizuhara, R. Mout, R. Das, S. T. Kim, Y.-C. Yeh, B. Yan, S. Hou, V. M. Rotello, *Nat. Chem.* **2015**, *7*, 597 – 603; f) A. M. Pérez-López, B. Rubio-Ruiz, V. Sebastián, L. Hamilton, C. Adam, T. L. Bray, S. Irusta, P. M. Brennan, G. C. Lloyd-Jones, D. Sieger, J. Santamaría, A. Unciti-Broceta, *Angew. Chem. Int. Ed.* **2017**, *56*, 12548 – 12552; *Angew. Chem.* **2017**, *129*, 12722 – 12726; g) M. A. Miller, B. Askevold, H. Mikula, R. H. Kohler, D. Pirovich, R. Weissleder, *Nat. Commun.* **2017**, *8*, 15906; h) B. J. Stenton, B. L. Oliveira, M. J. Matos, L. Sinatra, G. J. L. Bernardes, *Chem. Sci.* **2018**, *9*, 4185 – 4189; i) X. Wang, Y. Liu, X. Fan, J. Wang, W. S. C. Ngai, H. Zhang, J. Li, G. Zhang, J. Lin, P. R. Chen, *J. Am. Chem. Soc.* **2019**, *141*, 17133 – 17141; j) V. Sabatino, J. G. Rebelein, T. R. Ward, *J. Am. Chem. Soc.* **2019**, *141*, 17048 – 17052; k) M. Sancho-Albero, B. Rubio-Ruiz, A. M. Pérez-López, V. Sebastián, P. Martín-Duque, M. Arruebo, J. Santamaría, A. Unciti-Broceta, *Nat. Catal.* **2019**, *2*, 864 – 872; l) B. L. Oliveira, B. J. Stenton, V. B. Unnikrishnan, C. R. de Almeida, J. Conde, M. Negrão, F. S. S. Schneider, C. Cordeiro, M. G. Ferreira, G. F. Caramori, J. B. Domingos, R. Fior, G. J. L. Bernardes, *J. Am. Chem. Soc.* **2020**, *142*, 10869 – 10880; m) K. Vong, T. Yamamoto, T.-c. Chang, K. Tanaka, *Chem. Sci.* **2020**, https://doi.org/10.1039/D1030SC04329J; n) J. Chen, K. Li, J. S. L. Shon, S. C. Zimmerman, *J. Am. Chem. Soc.* **2020**, *142*, 4565 – 4569.

[10] a) R. M. Yusop, A. Unciti-Broceta, E. M. V. Johansson, R. M. Sánchez-Martín, M. Bradley, *Nat. Chem.* **2011**, *3*, 239 – 243; b) J. Clavadetscher, E. Indrigo, S. V. Chankeshwara, A. Lilienkampf, M. Bradley, *Angew. Chem. Int. Ed.* **2017**, *56*, 6864 – 6868; *Angew. Chem.* **2017**, *129*, 6968 – 6972; c) K. Tsubokura, K. K. H. Vong, A. R. Pradipta, A. Ogura, S. Urano, T. Tahara, S. Nozaki, H. Onoe, Y. Nakao, R. Sibgatullina, A. Kurbangalieva, Y. Watanabe, K. Tanaka, *Angew. Chem. Int. Ed.* **2017**, *56*, 3579 – 3584; *Angew. Chem.* **2017**, *129*, 3633 – 3638.

[11] a) S. Bose, A. H. Ngo, L. H. Do, *J. Am. Chem. Soc.* **2017**, *139*, 8792 – 8795; b) J. P. C. Coverdale, I. Romero-Canelón, C. Sanchez-Cano, G. J. Clarkson, A. Habtemariam, M. Wills, P. J. Sadler, *Nat. Chem.* **2018**, *10*, 347; c) Z. Du, C. Liu, H. Song, P. Scott, Z. Liu, J. Ren, X. Qu, *Chem* **2020**, *6*, 2060 – 2072.

[12] a) P. K. Sasmal, S. Carregal-Romero, A. A. Han, C. N. Streu, Z. Lin, K. Namikawa, S. L. Elliott, R. W. Koester, W. J. Parak, E. Meggers, *ChemBioChem* **2012**, *13*, 1116 – 1120; b) K. K. Sadhu, T. Eierhoff, W. Römer, N. Winssinger, *J. Am. Chem. Soc.* **2012**, *134*, 20013 – 20016; c) G. Thiabaud, R. McCall, G. He, J. F. Arambula, Z. H. Siddik, J. L. Sessler, *Angew. Chem. Int. Ed.* **2016**, *55*, 12626 – 12631; *Angew. Chem.* **2016**, *128*, 12816 – 12821; d) S. Alonso-de Castro, A. L. Cortajarena, F. López-Gallego, L. Salassa, *Angew. Chem. Int. Ed.* **2018**, *57*, 3143 – 3147; *Angew. Chem.* **2018**, *130*, 3197 – 3201; e) R. Huang, C.-H. Li, R. Cao-Milán, L. D. He, J. M. Makabenta, X. Zhang, E. Yu, V. M. Rotello, *J. Am. Chem. Soc.* **2020**, *142*, 10723 – 10729.

[13] a) J. Clavadetscher, S. Hoffmann, A. Lilienkampf, L. Mackay, R. M. Yusop, S. A. Rider, J. J. Mullins, M. Bradley, *Angew. Chem. Int. Ed.* **2016**, *55*, 15662 – 15666; *Angew. Chem.* **2016**, *128*, 15891 – 15895; b) J. Miguel-Ávila, M. Tomás-Gamasa, J. L. Mascareñas, *Angew. Chem. Int. Ed.* **2020**, *59*, 17628 – 17633; *Angew. Chem.* **2020**, *132*, 17781 – 17786.

[14] C. Vidal, M. Tomás-Gamasa, A. Gutiérrez-González, J. L. Mascareñas, *J. Am. Chem. Soc.* **2019**, *141*, 5125 – 5129.

[15] J. J. Hirner, Y. Shi, S. A. Blum, *Acc. Chem. Res.* **2011**, *44*, 603 – 613.

[16] a) A. S. K. Hashmi, C. Lothschütz, R. Döpp, M. Rudolph, T. D. Ramamurthi, F. Rominger, *Angew. Chem. Int. Ed.* **2009**, *48*, 8243 – 8246; *Angew. Chem.* **2009**, *121*, 8392 – 8395; b) W. M. Khairul, M. A. Fox, N. N. Zaitseva, M. Gaudio, D. S. Yufit, B. W. Skelton, A. H. White, J. A. K. Howard, M. I. Bruce, P. J. Low, *Dalton Trans.* **2009**, 610 – 620.

[17] a) S. M. Meier-Menches, B. Aikman, D. Döllerer, W. T. Klooster, S. J. Coles, N. Santi, L. Luk, A. Casini, R. Bonsignore, *J. Inorg. Biochem.* **2020**, *202*, 110844; b) J. Zhang, H. Zou, J. Lei, B. He, X. He, H. H. Y. Sung, R. T. K. Kwok, J. W. Y. Lam, L. Zheng, B. Z. Tang, *Angew. Chem. Int. Ed.* **2020**, *59*, 7097 – 7105; *Angew. Chem.* **2020**, *132*, 7163 – 7171.

[18] M. H. Pérez-Temprano, J. A. Casares, Á. R. de Lera, R. Álvarez, P. Espinet, *Angew. Chem. Int. Ed.* **2012**, *51*, 4917 – 4920; *Angew. Chem.* **2012**, *124*, 5001 – 5004.

[19] C. Vidal, M. Tomás-Gamasa, P. Destito, F. López, J. L. Mascareñas, *Nat. Commun.* **2018**, *9*, 1913.

[20] E. Indrigo, J. Clavadetscher, S. V. Chankeshwara, A. Megia-Fernandez, A. Lilienkampf, M. Bradley, *Chem. Commun.* **2017**, *53*, 6712 – 6715.
[21] S. Learte-Aymamí, C. Vidal, A. Gutiérrez-González, J. L. Mascareñas, *Angew. Chem. Int. Ed.* **2020**, *59*, 9149 – 9154; *Angew. Chem.* **2020**, *132*, 9234 – 9239.
[22] a) U. K. Marelli, F. Rechenmacher, T. R. A. Sobahi, C. Mas-Moruno, H. Kessler, *Front. Oncol.* **2013**, *3*, 00222; b) Y. Ma, G. Ai, C. Zhang, M. Zhao, X. Dong, Z. Han, Z. Wang, M. Zhang, Y. Liu, W. Gao, S. Li, Y. Gu, *Theranostics* **2017**, *7*, 1511 – 1523.

Manuscript received: October 4, 2020
Revised manuscript received: November 3, 2020
Accepted manuscript online: November 5, 2020
Version of record online: December 23, 2020

